Journal of information and communication convergence engineering
http://jicce.org

J. Inf. Commun. Converg. Eng. 15(4): 256-261, Dec. 2017 **Regular paper**

3D Visualization Technique for Occluded Objects in Integral Imaging Using Modified Smart Pixel Mapping

Min-Chul Lee[1], Jaeseung Han[2], and Myungjin Cho[2*], *Member, KIICE*

[1]Department of Computer Science and Electronics, Kyushu Institute of Technology, Fukuoka 820-8502, Japan
[2]Department of Electrical, Electronic, and Control Engineering, IITC, Hankyong National University, Anseong 17579, Korea

Abstract

In this paper, we propose a modified smart pixel mapping (SPM) to visualize occluded three-dimensional (3D) objects in real image fields. In integral imaging, orthoscopic real 3D images cannot be displayed because of lenslets and the converging light field from elemental images. Thus, pseudoscopic-to-orthoscopic conversion which rotates each elemental image by 180 degree, has been proposed so that the orthoscopic virtual 3D image can be displayed. However, the orthoscopic real 3D image cannot be displayed. Hence, a conventional SPM that recaptures elemental images for the orthoscopic real 3D image using virtual pinhole array has been reported. However, it has a critical limitation in that the number of pixels for each elemental image is equal to the number of elemental images. Therefore, in this paper, we propose a modified SPM that can solve this critical limitation in a conventional SPM and can also visualize the occluded objects efficiently.

Index Terms: Integral imaging, Modified smart pixel mapping, Occluded objects, 3D visualization

I. INTRODUCTION

Three-dimensional (3D) image sensing and visualization have been the most important techniques for many applications; unmanned autonomous vehicle system, biomedical imaging, the entertainment industry, defense applications, the 3D printing industry and so on. In particular, integral imaging first proposed by Lippmann [1] in 1908, can provide full color, full parallax, and continuous viewing points without any special glasses and coherent light sources. It can record multiple 2D images with different perspectives from 3D objects through a lenslet array. These images are called as elemental images. In the display stage, using these elemental images with the homogeneous lenslet array used in the pickup stage, a 3D image can be displayed. Fig. 1 illustrates the basic concept of integral imaging. However, the 3D image may have reverse depth information, a phenomenon called the pseudoscopic problem because of the lenslets and converging light field from the elemental images [2, 3]. To solve this problem, Okano et al. [4] proposed a method that rotates elemental images by 180 degree, a method called pseudoscopic-to-orthoscopic (PO) conversion. Thus, the pseudoscopic real 3D image can be easily converted by the orthoscopic virtual 3D image [5-10].

For the orthoscopic real 3D image display, PO conversion cannot work well. Thus, several studies [11-14] proposed a smart pixel mapping (SPM) technique that converts elemental images for the orthoscopic real 3D image display using virtual pinhole arrays. In this method, the assumption

Received 06 December 2017, **Revised** 13 December 2017, **Accepted** 20 December 2017
***Corresponding Author** Myungjin Cho (E-mail: mjcho@hknu.ac.kr, Tel: +82-31-670-5298)
Department of Electrical, Electronic, and Control Engineering, Hankyong National University, 327 Chungang-ro, Anseong 17579, Korea.
Min-Chul Lee and Jaeseung Han equally contributed to this work.

Open Access **https://doi.org/10.6109/jicce.2017.15.4.256** print ISSN: 2234-8255 online ISSN: 2234-8883

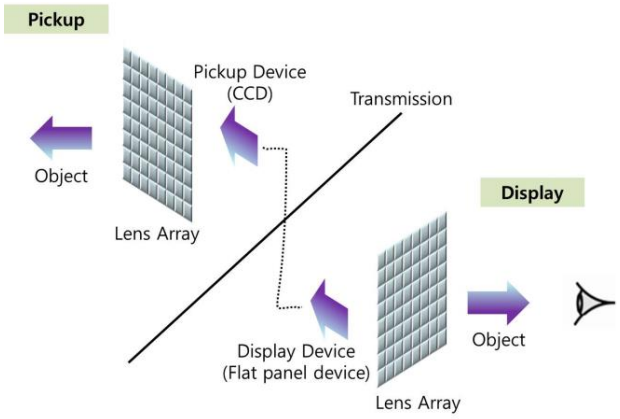

Fig. 1. Basic concept of integral imaging.

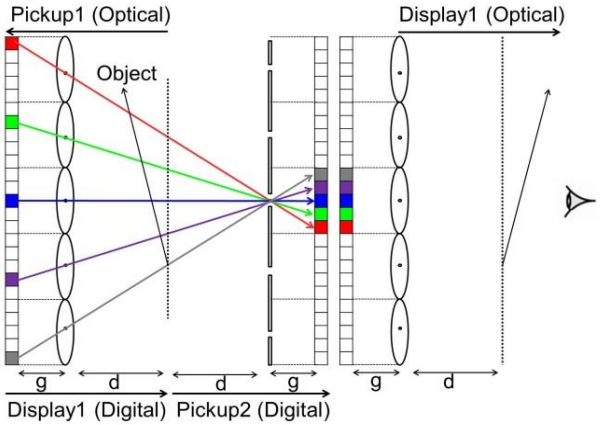

Fig. 2. Concept of conventional smart pixel mapping.

that the number of pixels for each elemental image is equal to the number of elemental images should be satisfied. This may be a critical limitation for various applications. To solve this problem and to visualize the occluded objects [15-19], we propose a modified SPM method herein.

The paper is organized as follows. In Section II, we describe the conventional SPM and our proposed SPM. Then, we show and discuss the experimental results to support our proposed method in Section III. Finally, we conclude with the summary in Section IV.

II. SMART PIXEL MAPPING

A. Conventional SPM

In conventional SPM, the most critical assumption is that the number of pixels for each elemental image is the same as the number of elemental images. Fig. 2 shows the concept of conventional SPM.

In "Pickup1," as shown in Fig. 2, each elemental image can be recorded optically by a lenslet array. Subsequently, in conventional integral imaging, through "Display1," pseudoscopic real 3D images that have reverse depth information can be displayed. Thus, in conventional SPM, pseudoscopic real 3D image can be reconstructed digitally, subsequently, using the virtual pinhole array, new elemental images are generated digitally in "Pickup2," as shown in Fig. 2. Finally, using the lenslet array, the orthoscopic real 3D image can be displayed in "Display2," as shown in Fig. 2.

Fig. 3 illustrates the relationship between SPM and lenslet array, where N is the number of pixels for each elemental image, M is the number of elemental images, g is the gap between the lenslet array and elemental images, and $2d$ is the distance between the lenslet array and the virtual pinhole array.

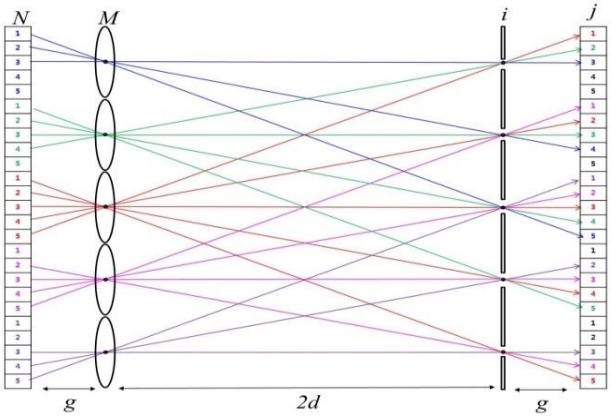

Fig. 3. Relationship between SPM and lenslet array.

For example, when $M = N = 5$, the 5th pixel by central virtual pinhole $D_{3,5}$ corresponds to the 1st pixel on the 1st elemental image $O_{1,1}$. Therefore, this pixel mapping relationship can be expressed as follows:

$$d = \frac{gM}{2}, \tag{1}$$

$$g = \frac{2d}{M}, \tag{2}$$

$$D_{i,j} = O_{k,l}, \tag{3}$$

$$k = i + \left(\frac{M+1}{2}\right) - j, \tag{4}$$

$$l = (M+1) - j, \tag{5}$$

where i,j are the indexes of the virtual pinhole and the regenerated elemental image pixel, respectively; k,l are the indexes of the lenslet and the elemental image pixel,

respectively. Using Eqs. (1)–(5), new elemental images for the orthoscopic real 3D image display can be generated. For example, when $k = 2$, $l = 4$, and $M = N = 5$, Eqs. (4) and (5) can be changed to $2 = i + 3 - j$ and $4 = 6 - j$, respectively. Thus, $i = 1$ and $j = 2$ can be obtained.

In "Display2," as shown in Fig. 2, using the new generated elemental images by Eqs. (1)–(5), the orthoscopic real 3D image can be displayed. However, conventional SPM should satisfy the critical assumption as mentioned before.

B. Modified SPM

In this paper, to solve the critical assumption of the conventional SPM, we propose a modified SPM technique. In our proposed SPM, Eqs. (4) and (5) can be modified as follows:

$$k = i + S\left(\frac{N+1}{2}\right) - j, \tag{6}$$

$$l = (N+1) - j, \tag{7}$$

where S is the depth plane for reconstruction.

Figs. 4 and 5 show the description of Eqs. (6) and (7), respectively. In Fig. 4, Eq. (6) can be obtained by the triangular geometry. In addition, Eq. (7) is derived by the triangular geometry, as shown in Fig. 5. Therefore, in our SPM method, the critical assumption of the conventional SPM no longer needs to be satisfied.

In our proposed method, the parameter S can have positive or negative values. When S is positive, the 3D image can be reconstructed in the real image field. However, when S is negative, the 3D image can be visualized in the virtual image field. Further, this parameter is of utmost importance for the visualization of the occluded objects in this paper because the reconstruction plane can be controlled by changing the value of this parameter.

In general, the pixel on the display panel is pixelated. According to the S value, the mapping relation of SPM may be incomplete. For example, all pixels are well mapped between two planes when SNg is an integer. Otherwise, the relation becomes incomplete. This means that the reconstructed image may have blank pixels, as shown in Fig. 6(a). To overcome this problem, we use the image interpolation process [20] for the blank pixels, as shown in Fig. 6(b).

To prove the ability for visualization of the occluded objects, Fig. 6 shows the reconstruction results using the conventional SPM and our proposed SPM. As shown in Fig. 6(b), our method can visualize the occluded objects more efficiently. However, the reconstructed 3D image by the conventional SPM as shown in Fig. 6(a) cannot visualize the occluded object because when the calculated k and l are out of the system range, the blank pixel is generated in the conventional SPM.

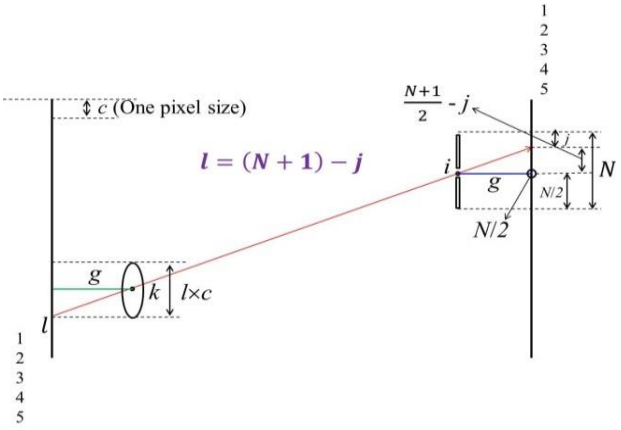

Fig. 4. Relationship between SPM and lenslet array.

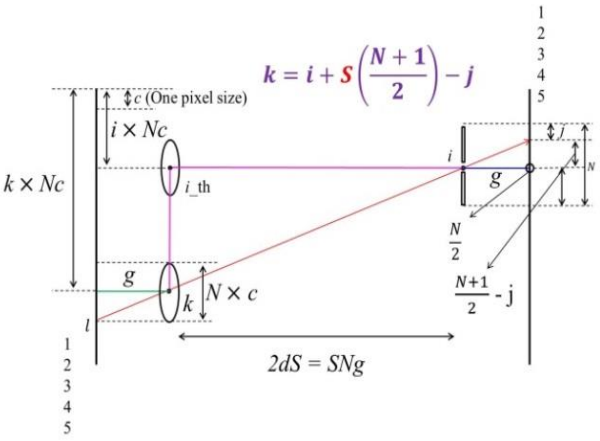

Fig. 5. Relationship between SPM and lenslet array.

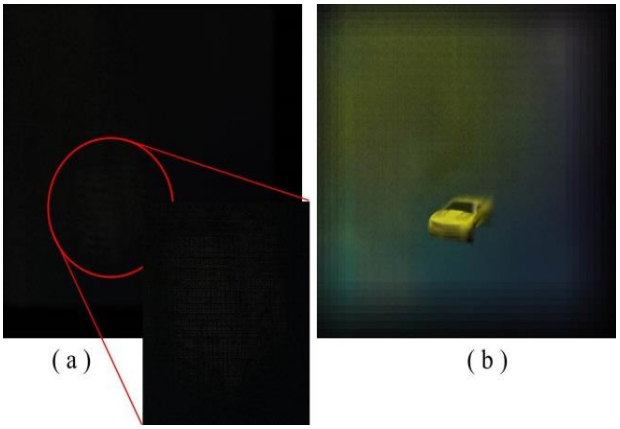

Fig. 6. Reconstructed 3D images by (a) the conventional SPM and (b) our proposed SPM.

III. EXPEROMENTAL RESULTS

To support our proposed method and to compare with the conventional SPM, we implement a computer simulation. Elemental images are obtained by the Unity 3D computer software as shown in Fig. 7. We capture 10(H) × 10(V) elemental images using a camera array. The resolution of each elemental image is 300(H) × 300(V). The focal length of the camera is 50 mm. The gap between the cameras is 2 mm. The occlusion part (tree) is positioned 50 mm from the camera array and the occluded object (car) is positioned 75 mm from the camera array.

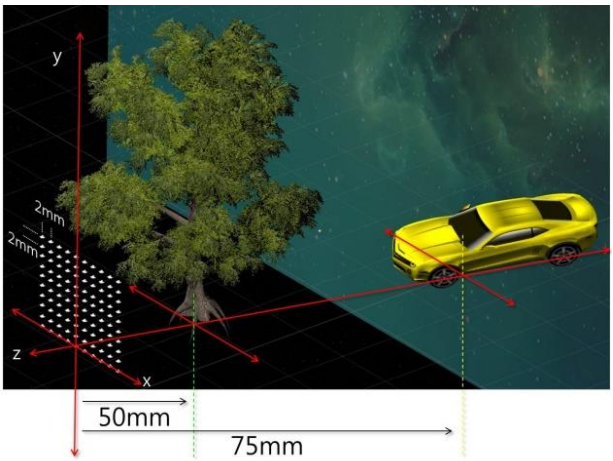

Fig. 7. Experimental setup.

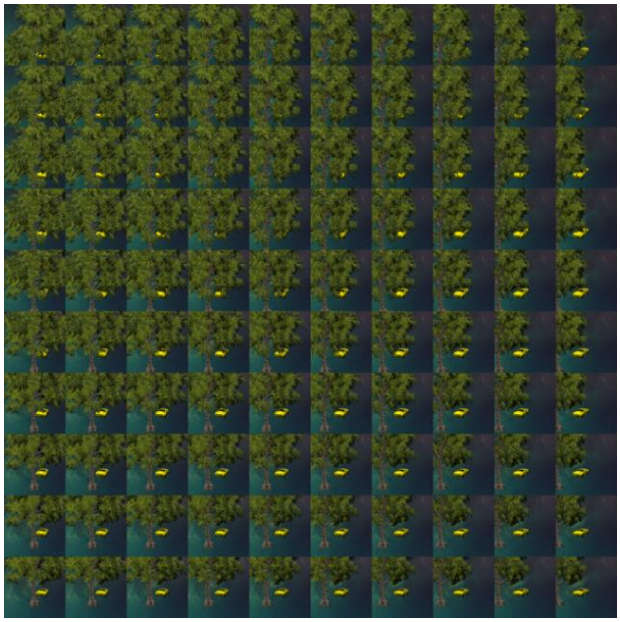

Fig. 8. Elemental images.

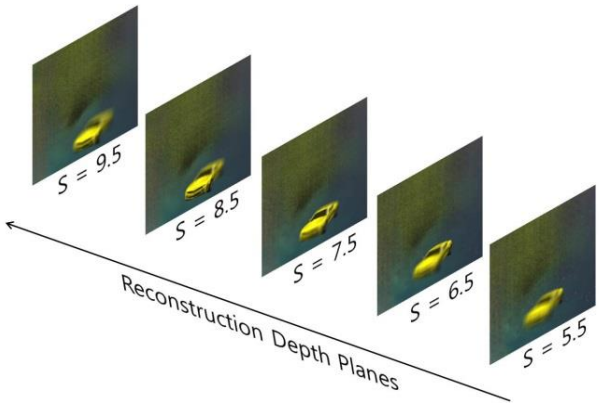

Fig. 9. Reconstruction results via various reconstruction planes using our proposed SPM method.

As the number of elemental images is 100 and each elemental image has 300(H) × 300(V) pixels, the total number of pixels for the elemental images set is 3000(H) × 3000(V). Fig. 8 shows the obtained elemental images by Unity 3D. We noticed that a certain elemental image cannot visualize the occluded object well.

As shown in Fig. 6(a) and (b), the conventional SPM cannot visualize the occluded object because it is used for PO conversion. However, our proposed method can reconstruct the occluded object since it uses the depth plane parameter S in the algorithm.

To show the ability of 3D reconstruction with our proposed method, we implement 3D reconstruction via various reconstruction depth planes, as shown in Fig. 9. We noticed that the clear reconstructed 3D image can be obtained when our proposed SPM method is implemented at the correct reconstruction depth plane (S = 85). However, when the reconstruction depth planes change, the reconstructed 3D image may have several blank pixels that may cause the low visual quality of the reconstructed 3D image.

To enhance the visual quality of the reconstructed 3D image using our proposed method, we used the image interpolation algorithm [20]. In fact, our method may generate blank pixels when the parameter S changes. Thus, to compensate these blank pixels, we use the bilinear interpolation method for the reconstructed 3D image. Fig. 10 shows the interpolation results for the reconstructed 3D image using our proposed SPM.

To evaluate the performance of our proposed method by comparing with the conventional SPM, we calculate the peak-signal-to-noise ratio (PSNR) as a performance metric. Tables 1 and 2 show the PSNR results via various reconstruction depth planes using conventional SPM and the modified SPM method with bilinear interpolation, respectively. It is shown that our proposed method has better reconstruction results than the conventional SPM. It is

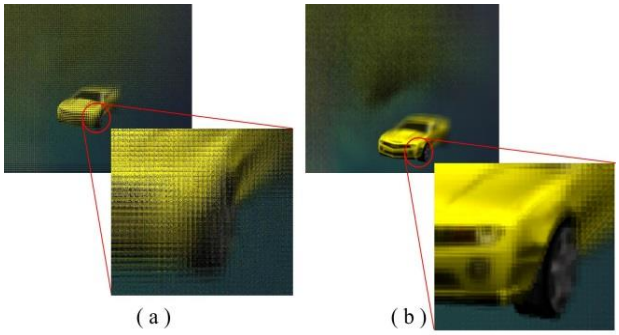

Fig. 10. Interpolation results: (a) without bilinear interpolation, (b) with bilinear interpolation.

Table 1. PSNR via various reconstruction depth planes from conventional SPM

	S = 75	S = 85	S = 95	S = 105	S = 115
Depth = 50	6.2290	6.2668	6.3160	6.3388	6.2852
Depth = 60	6.1781	6.2043	6.2186	6.2287	6.2256
Depth = 70	6.0350	6.0433	6.0534	6.0639	6.0736
Depth = 80	5.9667	5.9402	5.9484	5.9577	5.9339

Table 2. PSNR via various reconstruction depth planes from modified SPM and bilinear interpolation

	S = 75	S = 85	S = 95	S = 105	S = 115
Depth = 50	15.8568	16.9529	19.0531	27.4958	19.2841
Depth = 60	17.6534	26.9105	17.1381	16.1846	15.4867
Depth = 70	20.6039	11.6280	11.5673	11.6258	11.7705
Depth = 80	14.4301	7.8025	7.8458	7.8400	7.8984

possible to confirm that the PSNR of the image using the modified SPM formula and the bilinear interpolation is higher. Therefore, we prove that our proposed method in this paper is more effective. In addition, we noticed that PSNR difference becomes smaller when the reconstruction depth increases due to the depth resolution. In integral imaging, the depth resolution decreases when the reconstruction depth increases because the pixel shift of overlapped elemental images becomes smaller.

IV. CONCLUSIONS

In this paper, we have proposed a modified smart pixel mapping method to solve the critical assumption in the conventional SPM and to visualize the occluded objects. As our method does not have the critical assumption, it can be used for various applications. In addition, by changing the parameter *S* (i.e., reconstruction depth plane), the occluded objects can be visualized. However, several blank pixels occur when the parameter *S* changes in the occlusion environment, which may cause the low visual quality of the reconstructed 3D image. Using the interpolation method, we enhance the visual quality of the reconstructed 3D image. However, it is still a problem in our proposed method. For future work, we will investigate the new SPM method to reduce the blank pixels. In addition, we will develop a large 3D display system for the orthoscopic real 3D image.

ACKNOWLEDGMENTS

This study was supported by Basic Science Research Program through the National Research Foundation of Korea (NRF) funded by the Ministry of Education (No. NRF-2016R1E1A2A01952377).

REFERENCES

[1] G. Lippmann, “La photographie integrale,” *Comptes Rendus de l'Académie des Sciences*, vol. 146, pp. 446–451, 1908.

[2] R. Ng, M. Levoy, M. Bredif, G. Duval, M. Horowitz, and P. Hanrahan, “Light field photography with a hand-held plenoptic camera,” *Computer Science Technical Report*, vol. 2005, no. 2, pp. 1–11, 2005.

[3] R. Ng, “Digital light field photography,” Ph.D. dissertation, Stanford University, CA, 2006.

[4] F. Okano, H. Hoshino, J. Arai, and I. Yuyama, “Real-time pickup method for a three-dimensional image based on integral photography,” *Applied Optics*, vol. 36, no. 7, pp. 1598–1603, 1997.

[5] H. E. Ives, “Optical properties of a Lippmann lenticulated sheet,” *Journal of the Optical Society of America*, vol. 21, no. 3, pp. 171–176, 1931.

[6] N. Davies, M. McCormick, and L. Yang, “Three-dimensional imaging systems: a new development,” *Applied Optics*, vol. 27, no. 21, pp. pp. 4520–4528, 1988.

[7] H. Arimoto and B. Javidi, “Integral three-dimensional imaging with digital reconstruction,” *Optics Letters*, vol. 26, no. 3, pp. 157–159, 2001.

[8] Y. Hirayama, “One-dimensional integral imaging 3D display systems,” in *Proceedings of 3rd International Universal Communication Symposium (IUCS)*, Tokyo, Japan, pp. 141–145, 2009.

[9] S. H. Hong, J. S. Jang, and B. Javidi, “Three-dimensional volumetric object reconstruction using computational integral imaging,” *Optical Express*, vol. 12, no. 3, pp. 483–491, 2004.

[10] H. Yoo and D. H. Shin, “Improved analysis on the signal property of computational integral imaging system,” *Optics Express*, vol. 15, no. 21, pp. 14107–14114, 2007.

[11] M. Martinez-Corral, B. Javidi, R. Martinez-Cuenca, and G. Saavedra, “Formation of real, orthoscopic integral images by smart pixel mapping,” *Optics Express*, vol. 13, no. 23, pp. 9175–9180, 2005.

[12] J. H. Jung, J. Kim, and B. Lee, "Solution of pseudoscopic problem in Integral Imaging for real-time processing," *Optics Letters*, vol. 38, no. 1, pp. 76–78, 2013.

[13] Y. Piao, M. Zhang, J. J. Lee, D. Shin, and B. G. Lee, "Orthoscopic integral imaging display by use of the computational method based on lenslet model," *Optics and Lasers in Engineering*, vol. 52, pp. 184–188, 2014.

[14] M. Zhang, Y. Piao, and E. S. Kim, "Occlusion-removed scheme using depth-reversed method in computational integral imaging," *Applied Optics*, vol. 49, no. 14, pp. 2571–2580, 2010.

[15] B. Javidi, R. Ponce-Diaz, and S. H. Hong, "Three-dimensional recognition of occluded objects by using computational integral imaging," *Optics Letters*, vol. 31, no. 8, pp. 1106–1108, 2006.

[16] S. H. Hong and B. Javidi, "Distortion-tolerant 3D recognition of occluded objects using computational integral imaging," *Optics Express*, vol. 14, no. 25, pp. 12085–12095, 2006.

[17] M. Cho and B. Javidi, "Three-dimensional tracking of occluded objects using integral imaging," *Optics Letters*, vol. 33, no. 23, pp. 2737–2739, 2008.

[18] D. H. Shin, B. G. Lee, and J. J. Lee, "Occlusion removal method of partially occluded 3D object using sub-image block matching in computational integral imaging," *Optics Express*, vol. 16, no. 21, pp. 16294–16304, 2008.

[19] B. G. Lee and D. H. Shin, "Enhanced computational integral imaging system for partially occluded 3D objects using occlusion removal technique and recursive PCA reconstruction," *Optics Communications*, vol. 283, no. 10, 2084–2091, 2010.

[20] D. H. Shin and H. Yoo, "Image quality enhancement in 3D computational integral imaging by use of interpolation methods," *Optics Express*, vol. 15, no. 19, pp. 12039–12049, 2007.

Min-Chul Lee
received the B.S. degrees in Telecommunication Engineering from Pukyong National University, Busan, Korea, in 1996, and the M.S. and Ph.D. degrees from Kyushu Institute of Technology, Fukuoka, Japan, in 2000 and 2003, respectively. He is an assistant professor at Kyushu Institute of Technology in Japan. His research interests include medical imaging, blood flow analysis, 3D display, 3D integral imaging, and 3D biomedical imaging.

Jaeseung Han
received the B.S. in Computer Science and Multimedia Engineering from Dongseo University, Busan, Korea, in 2016. He is currently a master student at Hankyong National University in Korea. His research interests include 3D display, 3D reconstruction, and 3D integral imaging.

Myungjin Cho
received the B.S. and M.S. degrees in Telecommunication Engineering from Pukyong National University, Busan, Korea, in 2003 and 2005, and the M.S. and Ph.D. degrees in electrical and computer engineering from the University of Connecticut, Storrs, CT, USA, in 2010 and 2011, respectively. Currently, he is an associate professor at Hankyong National University in Korea. He worked as a researcher at Samsung Electronics in Korea, from 2005 to 2007. His research interests include 3D display, 3D signal processing, 3D biomedical imaging, 3D photon counting imaging, 3D information security, 3D object tracking, 3D underwater imaging, and 3D visualization of objects under inclement weather conditions.